Journal of Cellular Biochemistry 85:131–145 (2002)
DOI 10.1002/jcb.10100

Overexpression of Murine Phosphatidylinositol 4-Phosphate 5-Kinase Type Iβ Disrupts a Phosphatidylinositol 4,5 Bisphosphate Regulated Endosomal Pathway

Floyd J. Galiano,[1] Emin T. Ulug,[2] and J. Nathan Davis[1]*

[1]Department of Biochemistry and Molecular Biology and the Feist-Weiller Cancer Center, Louisiana State University Health Sciences Center, School of Medicine in Shreveport, Shreveport Louisiana 71130
[2]Department of Microbiology, University of Texas at Austin, Austin, Texas, 78712

Abstract The type I phosphatidylinositol 4-phosphate 5-kinases (PI4P5K) phosphorylate phosphatidylinositol 4-phosphate [PI(4)P] to produce phosphatidylinositol 4,5-bisphosphate [PI(4,5)P_2]. PI(4,5)P_2 has been implicated in signal transduction, receptor mediated endocytosis, vesicle trafficking, cytoskeletal structure, and membrane ruffling. However, the specific type I enzymes associated with the production of PI(4,5)P_2 for the specific cellular processes have not been rigorously defined. Murine PI4P5K type Iβ (mPIP5K-Iβ) was implicated in receptor mediated endocytosis through the isolation of a truncated and inactive form of the enzyme that blocked the ligand-dependent downregulation of the colony-stimulating factor-1 receptor. The present study shows that enforced expression of mPIP5K-Iβ in 293T cells resulted in the accumulation of large vesicles that were linked to an endosomal pathway. Similar results were obtained after the expression of the PI(4,5)P_2-binding pleckstrin homology (PH) domain of phospholipase-Cδ (PLC-δ). Analysis of the conserved domains of mPIP5K-Iβ led to the identification of dimerization domains in the N- and C-terminal regions. Enforced expression of the individual dimerization domains interfered with the proper subcellular localization of mPIP5K-Iβ and the PLC-δ-PH domain and blocked the accumulation of the endocytic vesicles induced by these proteins. In addition to regulating early steps in endocytosis, these results suggest that mPIP5K-Iβ acts through PI(4,5)P_2 to regulate endosomal trafficking and/or fusion. J. Cell. Biochem. 85: 131–145, 2002. © 2002 Wiley-Liss, Inc.

Key words: phosphatidylinositol 4-phosphate 5-kinase; phosphatidylinositol 4,5-bisphosphate; endocytosis; vesicles; PIP5K; PII domain; membrane trafficking

Phosphatidylinositol (PI) metabolism supplies crucial regulatory molecules for diverse cellular processes including signal transduction, endocytosis, vesicle trafficking, and the dynamics of cytoskeletal structure [Hinchliffe et al., 1998; Itoh et al., 2001]. The ability of phosphatidylinositol metabolism to contribute to these diverse functions results in part from the independent phosphorylation of the D-3, D-4, and D-5 positions of the inositol moiety. Position-specific kinases and phosphatases cooperate to generate all possible combinations of mono-, di-, and, tri-phosphorylated PI species. To begin to elucidate these complex regulatory pathways, biological roles must be assigned to these various enzymes.

Phosphatidylinositol 4,5-bisphosphate [PI(4,5)P_2] has been implicated in a variety of cellular processes, but its role in multiple steps of receptor mediated endocytosis is well documented. PI(4,5)P_2 acts early in endocytosis through the regulation of clathrin coat formation. Clathrin coats can be assembled onto

Grant sponsor: NIH (to E.T.U.); Grant number: CA58291; Grant sponsor: National Science Foundation (to J.N.D.); Grant number: MCB-9982410; Grant sponsor: Department of Biochemistry and Molecular Biology and the Feist-Weiller Cancer Center at Louisiana State Health Sciences Center, Medical School in Shreveport.

*Correspondence to: J. Nathan Davis, Department of Biochemistry and Molecular Biology and the Feist-Weiller Cancer Center, Louisiana State University Health Sciences Center, School of Medicine in Shreveport, Shreveport LA 71130. E-mail: ndavis@lsuhsc.edu

Received 17 September 2001; Accepted 19 November 2001

© 2002 Wiley-Liss, Inc.

$PI(4,5)P_2$-containing vesicles in vitro with the addition of the endocytic proteins, epsin or adaptor protein 180 (AP180), and adaptor protein 2 (AP2) [Ford et al., 2001; Itoh et al., 2001]. One current model suggests that $PI(4,5)P_2$ binding by epsin and AP180 recruits clathrin to the membrane and allows AP2 to stimulate coated pit formation in a $PI(4,5)P_2$ dependent manner [Gillooly and Stenmark, 2001]. Additionally, $PI(4,5)P_2$ is required in the formation of endocytic vesicles. By stimulating the GTPase activity of dynamin, a G-protein that rings the neck of the budding vesicle and is intimately tied to vesicle scission, $PI(4,5)P_2$ regulates the formation of the primary endosome [Tuma et al., 1993]. Since $PI(4,5)P_2$ is required at multiple steps early in the endocytic process, receptor mediated endocytosis provides a convenient system to dissect the enzymes involved in $PI(4,5)P_2$ synthesis.

The majority of cellular $PI(4,5)P_2$ is generated from phosphatidylinositol 4-phosphate [PI(4)P] formed by the action of phosphatidylinositol 4-kinase (PI4K) on PI. PI(4)P is converted to $PI(4,5)P_2$ through the activity of the type I phosphatidylinositol 4-phosphate 5-kinases (PI4P5K) which exists in three isoforms (α, β, and γ) [Ishihara et al., 1996; Loijens et al., 1996; Ishihara et al., 1998]. Type I PI4P5Ks also participate in an alternate route of $PI(4,5)P_2$ synthesis by directly utilizing PI as a substrate to yield phosphatidylinositol 5-phosphate [PI(5)P] [Rameh et al., 1997]. PI(5)P can then be converted to $PI(4,5)P_2$ by one of three isoforms of the type II phosphatidylinositol 5-phosphate 4-kinases (PI5P4K). Since the type I PI4P5Ks are required for the synthesis of $PI(4,5)P_2$ by both synthetic routes, these enzymes present a pivotal point for regulation by the cell.

The type I and II phosphatidylinositol phosphate kinases constitute a kinase subfamily and share appreciable primary sequence identity that is divergent from other kinase families [Hinchliffe et al., 1998; Rao et al., 1998]. However, the crystal structure of PI5P4K-II β shows structural motifs conserved to the kinase superfamily [Rao et al., 1998]. Like all kinases, the ATP-binding site of PI5P4K-II β resides in a cleft formed between N-terminal and C-terminal globular domains. The tertiary structure of PI5P4K-II β consists of a homodimer with the dimerization face present on the N-terminal globular domain. The C-terminal domain contains a disordered loop that is topologically analogous to the activation loop of other kinases. Domain swap experiments that placed the type I activation loop in the context of the type II enzyme demonstrated that this activation loop was sufficient to determine substrate specificity [Kunz et al., 2000]. The resulting chimera displayed type I enzyme activity in vitro by utilizing PI(4)P to produce $PI(4,5)P_2$ and in vivo by regulating the actin cytoskeleton structure. Thus, the amino terminal domain of these enzymes is involved in protein dimerization while the C-terminal domain determines substrate specificity and enzyme regulation.

Only the type I PI4P5Ks have been associated with membrane trafficking, and only the β-isoform has been directly implicated in receptor mediated endocytosis. The β-isoform of the type I murine phosphatidylinositol 4-phosphate 5-kinase (mPIP5K-Iβ) was implicated in receptor tyrosine kinase (RTK) trafficking through a genetic screen designed to identify effector molecules capable of complementing a mitogenically defective colony stimulating factor-1 receptor [CSF-1R (Phe809)] [Davis et al., 1997]. Truncation of the first 238 amino acids of mPIP5K-Iβ produced an enzymatically inactive protein (mPIP5K-Iβ 1-238) that blocked ligand dependent degradation and restored CSF-1 dependent proliferation to cells expressing CSF-1R(Phe809). These results suggested that mPIP5K-Iβ $\triangle$1-238 functioned as a dominant-negative inhibitor to block mPIP5K-Iβ regulation of RTK trafficking. More recently, it was shown that mPIP5K-Iβ overexpression decreased the ATP sensitivity of inward rectifying potassium channels (K_{ATP}) while overexpression of mPIP5K-Iβ $\triangle$1-238 increased the ATP sensitivity of these channels [Shyng et al., 2000]. These observations are consistent with previous work showing that ATP inhibition of K_{ATP} channels was reversible by $PI(4,5)P_2$. The observation that mPIP5K-Iβ $\triangle$1-238 is antagonistic to mPIP5K-Iβ regulated activities supports the hypothesis that mPIP5K-Iβ $\triangle$1-238 functions as a dominant negative.

While mPIP5K-Iβ is involved in the early stages of receptor mediated endocytosis, the enzyme could also be required at later steps required for proper receptor trafficking, such as targeting of the activated RTK or endocytic vesicle trafficking. This report provides evidence that mPIP5K-Iβ is involved in regulating endosomal vesicle trafficking. Enforced expression of wild type and kinase-dead forms

of mPIP5K-Iβ in 293T cells resulted in the accumulation of large vesicles linked to an endocytic pathway. Deletion analysis of mPIP5K-Iβ demonstrated that the entire kinase core domain was required for the accumulation of the large vesicles and lead to the identification of two dimerization domains within the protein. mPIP5K-Iβ, like the type II PI5P4Ks, contains a dimerization domain in an N-terminal region but mPIP5K-Iβ contains an additional dimerization domain in the C-terminus. Co-expression of mPIP5K-Iβ with the isolated N- and C-terminal regions inhibited mPIP5K-Iβ induced accumulation of endocytic vesicles and altered the subcellular distribution of mPIP5K-Iβ. Expression of PI(4,5)P_2-binding pleckstrin homology (PH) domain derived from phospholipase Cδ (PLC-δ) in 293T cells induced the accumulation of large vesicles in a manner similar to mPIP5K-Iβ and mPIP5K-Iβ co-localized with the PLC-δ-PH on the plasma membrane. Thus, the accumulation of the large vesicles was associated with the expression of proteins that possess the potential to disrupt PI(4,5)P_2 metabolism.

MATERIALS AND METHODS

Cell Lines

293T cells were grown in Dulbecco's modification of minimal essential media (Cellgro) supplemented with 10% fetal bovine serum (Biowhittaker), 100 U of pencillin/streptomycin (Cellgro) and maintained at 37°C in an atmosphere of 5% CO_2. Cells were transfected by using a modified calcium phosphate precipitation procedure as previously described [Chen and Okayama, 1987].

Plasmids

All cDNA constructs were prepared in the pcDNA 3.1 expression vector (Invitrogen). pcDNAmPIP5K-Iβ construction was previously described [Davis et al., 1997]. Construction of the mPIP5K-Iβ K179M and mPIP5K-Iβ D244V point mutations was performed using the polymerase chain reaction (PCR). The sequence of the 5′ primer for the construction of the K179M mutation was 5′-GATGAATTCATCATTATG-ACCGTCC-3′ and the 3′ primer was 5′-GAG-AGAATTCCTTCTGAGGCTCACTGCTCAG-3′. For construction of the D244V mutation, the 5′primer sequence was 5′-GAATGCATATGA-AATATGTCCTGAAG-3′ and the 3′primer described above. The fragments containing the mutations were amplified using Taq polymerase (Stratagene) using manufacturer's instructions and cloned into the TA cloning system (Invitrogen). The fragments containing the mutations were inserted into the wild-type sequence using the Eco RI (for K179M) or Nde I (for D244V) restriction endonuclease digestion sites. Fusion of the fluorescent proteins was at the amino terminus of mPIP5K-Iβ, mPIP5K-Iβ △1-238, and mPIP5K-Iβ 1-149. The fusion constructs were prepared by using PCR to amplify the coding sequences of the fluorescent proteins with a Bgl II restriction endonuclease digestion site in the appropriate reading frame at the 3′-end of the amplified fluorescent protein coding sequence. For fusion to mPIP5K-Iβ and mPIP5K-Iβ 1-149 the primer sequences were 5′-GAGAGGATCCGTCGACCATGGTGAGCA-AGGGCGAG-3′ and 5′-GAGATCTAGATAGAT-CTCTTGTACAGCTCGTCCATGCC-3′ and for mPIP5K-Iβ △1-238 the above 5′primer was paired with the 3′ primer with the sequence of 5′-GAGATCTAGATGAGATCTTTCTTGTA-CAGCTCGTCC-3′. Construction of mPIP5K-Iβ 1-149 was performed using PCR, and the sequences of the primers are the following: 5′-GAGAGGATCCGCCAAGATGGCGTCCGC-3′ and 5′-GAGATCTAGAGGGAGTACAAGTA-ATCA-3′. The fragments encoding the fluorescent proteins were digested with the restriction endonucleases Bam HI and Bgl II and inserted into Bam HI digested mPIP5K-Iβ, mPIP5K-Iβ △1-238 and mPIP5K-Iβ 1-149. The nucleotide sequence of all the PCR products was confirmed by DNA sequencing at the Iowa State University DNA Sequencing and Synthesis Facility (Ames, Iowa), and the sequence was analyzed using the Wisconsin GCG DNA sequence analysis software.

The green fluorescent protein (GFP) tagged pleckstrin homology domains from phospholipase C-δ (PLC-δ-PH) and Brutons tyrosine kinase (BTK-PH) were previously described [Varnai et al., 1999]. The GFP-PLC-δ point mutation was previously described [Kost et al., 1999]. For construction of the cyan or yellow fluorescent protein (CFP or YFP) tagged versions of PLC-δ-PH and BTK-PH, the coding sequences for CFP or YFP were generated by PCR using the primers described above for GFP. The CFP or YFP coding sequence was substituted for that of GFP, and the entire cDNA was cloned into the pcDNA 3.1 vector.

Antibodies, Western Analysis, and Immunoprecipitation

Antibodies specific to mPIP5K-Iβ or GFP were produced in New Zealand White rabbits using bacterially expressed protein. The full-length mPIP5K-Iβ cDNA was cloned into pQE 30 (Qiagen) and the GFP cDNA was cloned into the pET (Stratagene) bacterial expression vector. The proteins were purified over Ni-agarose (Qiagen) either under denaturing conditions for mPIP5K-Iβ or non-denaturing conditions for GFP as per manufacturer's instructions. The proteins were injected (250 μg per immunization) in Titermax adjuvant monthly and antiserum collected by the Animal Resource Center at Louisiana State University Health Sciences Center Medical School in Shreveport. Antibody titers were followed using Western analysis of bacterially expressed protein and cell extracts prepared from transfected cells.

Western analysis was performed essentially as previously described [Burnette, 1981]. Extracts of transfected or control cells were prepared after scraping the cells into Tris buffered saline (TBS). The cells were collected by centrifugation and lysates were prepared by the addition of Laemmli's SDS–PAGE loading buffer [Laemmli, 1970], and the DNA sheared by sonication. The lysates were clarified by centrifugation in a refrigerated microcentrifuge at 13,000 rpm for 15 min. The proteins in the lysates were separated using SDS–PAGE and transferred to nylon reinforced nitrocellulose membranes (MSI). The membranes were blocked by incubation in TBS with 5% nonfat dry milk for 1 h at room temperature. The antiserum was added at a 1:250 dilution in TBS with 5% nonfat dry milk for 1 h at room temperature. After incubation with the primary antibody, the membrane was washed once with TBS, twice with TBS plus 0.1% Tween-20, and once with TBS for 5 min each at room temperature. The secondary antibody employed was alkaline phosphatase conjugated affinity purified goat anti-rabbit (Bio-Rad) diluted 1:2,000 in TBS with 5% nonfat dry milk and incubated for 1 h at room temperature. The membrane was washed as before and developed using the Immunstar Kit (Bio-Rad) according to manufacturer's instructions.

For immunoprecipitations, the transfected or control cells were scraped into PBS and collected by centrifugation. Cell lysates were prepared by triturating the cells in immunoprecipitation (IP) buffer (25 mM Tris pH 7.5, 0.5% Triton X-100, 100 mM NaCl, 100 kallikrein inhibitory units of aprotinin/milliliter and 0.2 mM phenylmethylsulfonyl fluoride), and the lysates clarified by centrifugation at 13,000 rpm in a refrigerated microcentrifuge. The clarified lysates were aliquoted to microcentrifuge tubes containing 7 μl of either immune or preimmune serum and the total volume of the reaction adjusted to 700 μl with IP buffer. After incubation at 4°C for 1 h with constant agitation, 30 μl of a 50% slurry of Protein-A Sepharose (Sigma) that was suspended in IP buffer was added and the reaction returned to 4°C for 30 min. The Protein-A Sepharose beads were collected by centrifugation in a microcentrifuge at top speed for 30 s and the supernatant was aspirated. The beads were washed three times with 1 ml IP buffer.

Kinase Assays

Immune complex PIP5-kinase activity was measured in vitro using conditions described previously [Ulug et al., 1990]. Immunoprecipitates were formed using 0.2 mg 293T cell protein and antiserum to PIP5K or GFP. PI 5-kinase assays were performed with total reaction volumes of 20 μl, containing 20 mM Hepes (pH 7.4), 5 mM $MgCl_2$, 2.5 mM dithiothreitol, 5 μg lipid substrate, and 10 mM [γ-^{32}P]ATP. Substrate for these assays contained a sonicated mixture of phosphoinositide and phosphatidylserine at a ratio of 1:3 (wt/wt). PIP used in these reactions was either derived from Brain (Sigma P-9638) or synthetically generated with phosphate at the D-3, D-4, or D-5 positions (Echelon Research Laboratories, Salt Lake City). PIP[γ-^{32}P]ATP was diluted with unlabeled ATP to a specific radioactivity of 5–10 μCi per 20 pmol reaction. After incubation for 10 min at 30°C, reactions were terminated by addition of 180 μl 1 N HCl and 400 μl chloroform/methanol (1:1). Samples were mixed vigorously, and phases were separated by brief centrifugation. The lower organic phase was washed with 400 μl of methanol/1N HCl (1:1) and dried. Lipids were resuspended in 10 μl chloroform and spotted onto oxalate-impregnated, heat-activated silica chromatography plates. TLC utilized a solvent system containing chloroform/methanol/acetone/acetic acid/H_2O (60:20:23:18: 11). ^{32}P-labeled phosphoinositides

were identified by autoradiography, and their migration was compared with iodine-stained standards.

Immunofluorescence and Microscopy

For immunofluorescence, the 293T cells were plated on 22×22 cm coverslips. The cells were washed 16 h after transfection with pre-warmed culture media and the coverslips were distributed to a 6-well plate. The cells were washed in PBS and incubated in 2% formaldehyde in PBS for 5 min at room temperature. After one wash with PBS, the cells were incubated with 99% methanol with 1% formaldehyde at -20°C for 5 min and then the cells were washed four times in PBS. The non-immune or PIP5K-Iβ immune serum was diluted 1:250 in BSP (2.5 mg/ml bovine serum albumin, 1 mg/ml saponin in PBS), and incubated for 1.5 h at room temperature. After four washes with PBS, the fluorescien isothiocyanate-conjugated goat anti-rabbit secondary antibody (Jackson Laboratories) diluted 1:100 in BSP was added and incubated for 1.5 h at room temperature. The cells were washed four times in PBS and the coverslips mounted on pre-cleaned glass slides in 0.5% *p*-phenylenediamine in 90% glycerol and sealed with clear nail polish.

For labeling of the cells with fluorescien isothiocyanate conjugated dextran (Sigma) or Texas-red conjugated transferrin (Molecular Probes), the cells were plated on 22×22 cm coverslips. The cells were washed 16 h after transfection with pre-warmed culture media and distributed to a 6-well plate. The fluorescien isothiocyanate conjugated dextran (10 mg/ml) or Texas-red conjugated transferrin (100 μg/ml) was diluted into pre-warmed media and incubated at 37°C for 1 h. The cells were washed with pre-warmed culture media and the coverslips mounted on glass slides as wet mounts.

Fluorescence was detected using an Olympus-AX-70 epifluorescence microscope e-quipped with differential interference optics. Monochrome images were captured at the microscope using a cooled-CCD camera (Nu 200: Princeton Instruments) and IP-Lab software (Scanalytics, Inc.) run on an Apple G4 computer. Images of the yellow and cyan GFP-variants were captured using the JP4 dual band filter set (Chroma Technology Corp).

RESULTS

Enforced Expression of mPIP5K-Iβ in 293T Cells Disrupts Endosomal Trafficking

In order to analyze the biological role of mPIP5K-Iβ, site directed mutagenesis was performed to generate kinase inactive isoforms of the enzymes. Two residues were selected for mutagenesis, lysine-179 (K179) and aspartic acid-244 (D244). K179 corresponds to the conserved lysine in the ATP binding pocket of all kinases and was converted to methionine (M) [Rao et al., 1998]. M substitution for K179 resulted in mPIP5K-Iβ K179M previously shown to produce a kinase inactive isoform [Ishihara et al., 1996]. D244, which lies in a domain equivalent to one proposed to function in substrate-binding for PI4P5K-IIβ [Rao et al., 1998], was converted to valine (V) to form mPIP5K-Iβ D244V. Evaluation of the enzyme activity of the mPIP5K wild-type (wt) and variant forms was determined after enforced expression in 293T cells. Cell extracts were prepared from the transfected cells and the expression of the proteins was confirmed by Western blot analysis with an antiserum to the amino-terminus of mPIP5K-Iβ (Fig. 1 panel A). The level of overexpression obtained in the transfection could not be precisely determined by Western analysis since the endogenous protein could not be readily detected. Immune complex kinase assays demonstrated increased lipid kinase activity only in the extracts containing mPIP5K-Iβ wt, despite equivalent levels of expression of mPIP5K-Iβ K179M and mPIP5K-Iβ D244V (Fig. 1 panel B). Overexposure of the chromatography plates allowed the detection of the endogenous kinase activity in the extracts prepared from the control cells and cells expressing mPIP5K-Iβ K179M and mPIP5K-Iβ D244V (data not shown).

Differential interference contrast (DIC) microscopy of the cells transfected with plasmids expressing mPIP5K-Iβ, mPIP5K-Iβ K179M and mPIP5K-Iβ D244V revealed the accumulation of large vesicles in the cytoplasm (Fig. 1C). This “large vesicle” phenotype was independent of kinase activity, since enforced expression of mPIP5K-Iβ K179M and mPIP5K-Iβ D244V resulted in the accumulation of the vesicles in the 293T cells. In contrast, transfection of 293T cells with vector alone or mPIP5K-Iβ expression vectors lacking an SV40 origin did not induce vesicle accumulation (data not

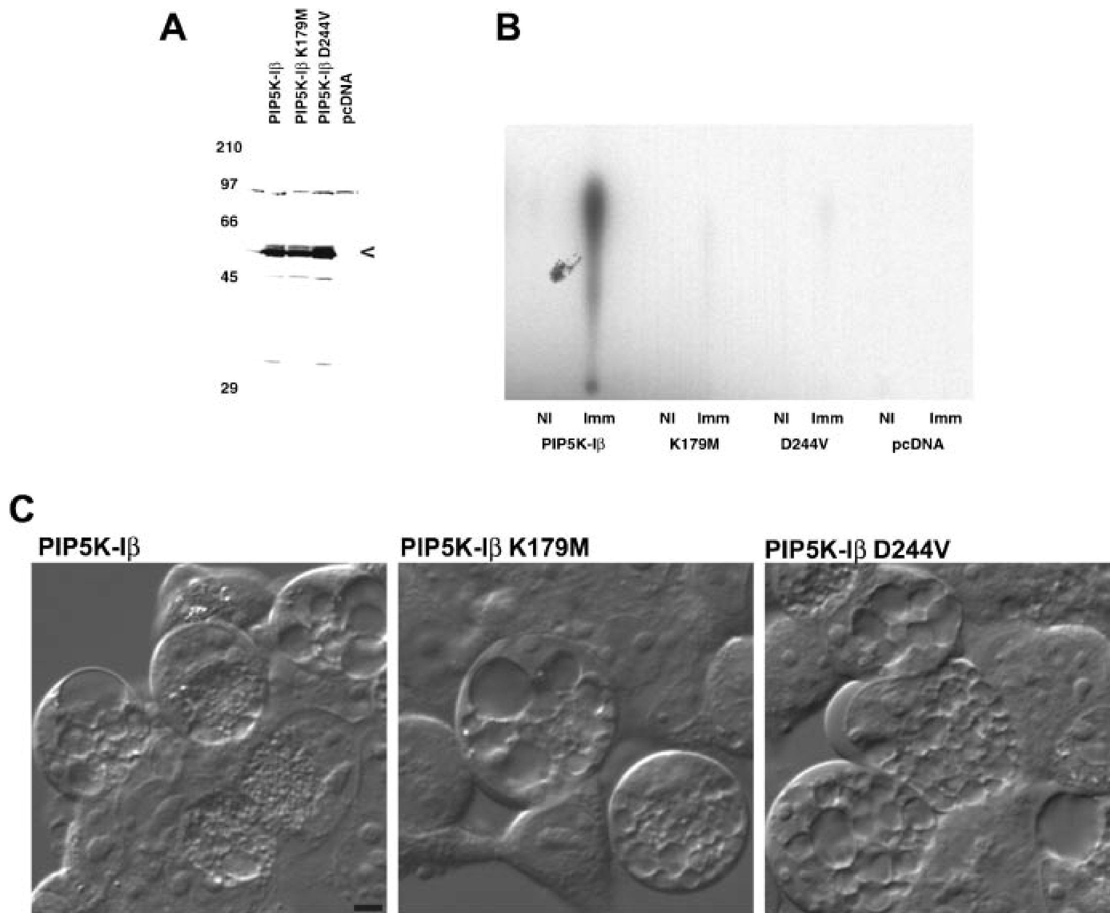

Fig. 1. Overexpression of mPIP5K-Iβ wild type and kinase-dead isoforms in 293T cells. **Panel A**: Western analysis of extracts prepared from 293T cells transfected with mPIP5K-Iβ, mPIP5K-Iβ K179M, mPIP5K-Iβ D244V expression vectors or with empty pcDNA as indicated. The molecular mass markers are shown in the first lane of the blot and masses are indicated on the side. The immunoreactive protein, mPIP5K-Iβ, is indicated by the arrow. **Panel B**: Autoradiogram of the phosphorylated products produced in immune complex kinase assays prepared from the cellular extracts analyzed in panel A as indicated below the radiogram. Either non-immune or mPIP5K-Iβ specific serum was used as indicated and PI (4) P purified from bovine brain was used as the substrate. The migration of the PI(4,5)P_2 is shown to the right. **Panel C**: Photomicrographs of 293T cells transfected with plasmids directing the synthesis of mPIP5K-Iβ, mPIP5K-Iβ K179M or mPIP5K-Iβ D244V. The photomicrographs were taken under 40 × magnification, and the magnification was digitally increased. The bar inserted into the first picture of panel A represents 10 μm.

shown). Additionally, transfection of the mPIP5K-Iβ expression plasmid into the 293 cells or NIH 3T3 cell lines, which can not support the episomal replication of the vector, did not induce the large vesicle phenotype. Thus, the large vesicle phenotype correlated with high level expression of mPIP5K-Iβ and may have resulted from the titration of important regulatory factors.

Indirect immunofluorescence studies of the transfected cells using antibodies raised against mPIP5K-Iβ revealed mPIP5K-Iβ expression in the cells displaying the accumulation of large vesicles (compare arrows in the left and right micrographs shown in panel A of Fig. 2). Anti-PIP5K-Iβ serum stained the plasma membrane as well as the surface of the large vesicles. The non-immune serum displayed no staining of the cells even though cells containing the large vesicles were present (Fig. 2B). The membrane localization of the kinase is consistent with previous biochemical studies which localized the type I PIP5K activity to the plasma membrane [Loijens et al., 1996]. To identify the origin of the large vesicles, transfected 293T cells were incubated with fluorescien isothiocyanate-dextran (FITC-dextran) as a marker for fluid phase uptake (Fig. 2, panel C) or rhodamine-transferrin (RITC-transferrin) as a marker for receptor mediated endocytosis (Fig. 2, panel D). Both the FITC-dextran and RITC-transferrin were localized to the large

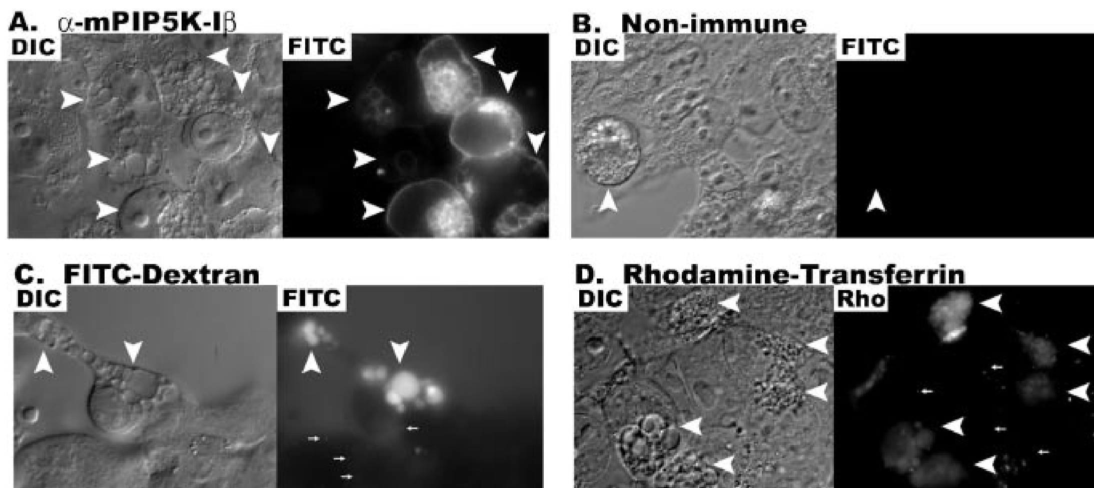

Fig. 2. mPIP5K-Iβ localized to the plasma membrane and the aberrant large vesicles that are associated with an endocytic pathway. **Panel A**: Photomicrographs of 293T cells expressing mPIP5K-Iβ analyzed by using differential contrast interference optics (DIC) or fluorescent microscopy (FITC) after staining with α-mPIP5K-Iβ antiserum and a FITC-labeled goat anti-rabbit secondary antibody. Arrowheads indicate transfected cells. **Panel B**: Photomicrographs of 293T cells expressing mPIP5K-Iβ analyzed by using differential contrast interference optics (DIC) or fluorescent microscopy (FITC) after staining with non-immune antiserum and a FITC-labeled goat anti-rabbit secondary antibody. Arrowheads indicate cells that have accumulated large vesicles. **Panel C**: Photomicrographs of 293T cells expressing mPIP5K-Iβ and incubated with fluorescien isothiocyanate-dextran (FITC-dextran) for 30 min prior to microscopy. The large arrowheads indicate cells expressing the large vesicle phenotype. The small arrows indicate the normal uptake of the FITC-dextran by non-transfected cells. **Panel D**: Photomicrographs of 293T cells expressing mPIP5K-Iβ and incubated with rhodamine conjugated transferrin (RITC-transferrin) for 30 min prior to microscopy. The large arrowheads indicate cells expressing the large vesicle phenotype. The small arrows indicate the normal uptake of the RITC-transferrin by non-transfected cells.

vesicles, indicating that these vesicles corresponded to endosomal components.

Enforced Expression of Phospholipase-C-δ Pleckstrin Homology Domain (PLC-δ-PH) in 293T Cells Disrupts Endosomal Trafficking

Since the disruption of the endosomal trafficking was dependent upon protein levels rather than enzyme activity, it was hypothesized that enforced expression of mPIP5K-Iβ was interfering with PI (4,5)P_2 metabolism. It was previously shown that the enforced expression of the mPIP5K and mPIP5K-Iβ △1-238 failed to induce significant changes in total cellular PI (4,5) P_2 [Davis et al., 1997]. Thus, the accumulation of the large vesicles may involve qualitative rather than quantitative changes in PI metabolism. The PH domain of PLC-δ (PLC-δ-PH) binds PI (4,5) P_2 with high affinity and enforced expression of PLC-δ-PH, as a GFP fusion, has been exploited to inhibit PI (4,5) P_2 dependent pathways and as a probe to observe changes in PI (4,5) P_2 pools in living cells [Stauffer et al., 1998; Varnai and Balla, 1998; Kost et al., 1999]. In contrast, the Bruton's tyrosine kinase PH domain (Btk-PH) binds PI (3,4,5) P_3 preferentially [Varnai et al., 1999]. Enforced expression of these PH domains was used to determine if the disruption of phosphatidylinositol pathways could induce the accumulation of large vesicles in the 293T cells.

Chimeric proteins combining YFP appended to the C-terminus of the PH domain of PLC-δ (YFP-PLC-PH) and to the C-terminus of the PH domain derived from Btk (YFP-Btk-PH) were obtained and transfected into the 293T cells. Cells expressing the YFP-PLC-δ-PH domain displayed an accumulation of endocytic vesicles that was strikingly similar to that of the cells expressing mPIP5K-Iβ (Fig. 3A). Like mPIP5K-Iβ, the YFP-PLC-δ-PH domain localized to the plasma membrane and to the surface of the large vesicles. The ability of the YFP-PLC-PH domain to induce vesicle accumulation correlated with its ability to bind PI (4,5) P_2, since a point mutation in the PH domain (YFP-PLC-δ-PH K32E) not only failed to properly localize to the plasma membrane but also failed to induce the large vesicle phenotype (Fig. 3B). The large vesicles induced by enforced expression of PI (4,5) P_2 were associated with an endocytic pathway, since the FITC-Dextran added to the media was transported into the vesicles

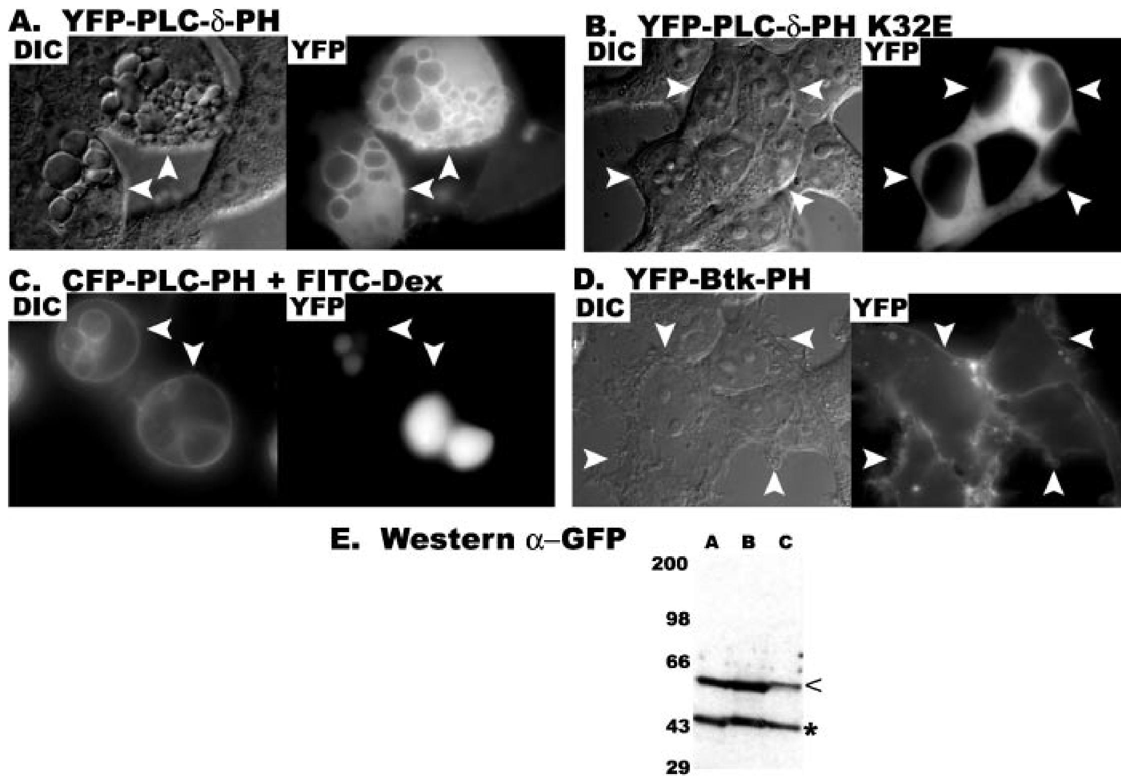

Fig. 3. Overexpression of the PI (4,5) P_2 binding PH-domain from PLC-δ in 293T cells induces the accumulation of large vesicles. **Panel A**: 293T cells were transfected with an expression vector encoding YFP- PLC-δ-PH and photographed by using DIC or fluorescent microscopy (YFP). **Panel B**: Photomicrographs of 293T cells expressing YFP-tagged PLC-δ-PH K32E which is unable to bind in PI (4,5) P_2. **Panel C**: 293T cells were transfected with the YFP-PLC-δ-PH vector and incubated with FITC-Dextran as a marker for fluid phase uptake. Photomicrographs were taken using the JP4 filter set designed to distinguish CFP from YFP fluorescence but also distinguishes CFP emission from FITC. **Panel D**: 293T cells were transfected with a vector that encodes the PI(3,4,5)P_3-binding YFP-Btk-PH domain and examined with DIC microscopy or fluorescent microscopy (YFP). **Panel E**: Autoradiogram from the Western blot analysis of proteins expressed in 293T cells transfected with the YFP-tagged PLC-δ-PH domain (a), YFP-tagged Btk-PH domain (b) or the YFP-tagged PLC-δ-PH K32E (c). The α-GFP serum was used in the Western blot analysis. An arrowhead designates the recombinant proteins and the nonspecific reactive band is indicated with the asterisk.

(Fig. 3C). By contrast, overexpression of the PI (3,4,5) P_3-binding PH domain of Btk failed to induce the accumulation of the large vesicles (Fig. 3D) indicating that the large vesicle phenotype was associated with disruption of PI (4,5) P_2 rather than PI (3,4,5) P_3 mediated pathways. These data indicate that, like mPIP5K-Iβ, the enforced expression of the PI (4,5) P_2-binding PLC-PH domain interferes with endosomal trafficking and leads to the accumulation of large endocytic vesicles.

mPIP5K-Iβ Contains Two Dimerization Domains

The accumulation of the large vesicles in cells expressing high levels of mPIP5K-Iβ could arise from the titration of a cellular factor(s) that are required for endosomal trafficking. To test this possibility, experiments were designed to define the domain(s) of mPIP5K-Iβ responsible for the large vesicle phenotype. To aid in the identification of transfected cells, constructs were made to encode green fluorescent protein (GFP) fused to the amino terminus of full-length or various mPIP5K-Iβ N- and C-terminal domains. Constructs were transfected into 293T cells, and protein expression was monitored by DIC and fluorescent microscopy. Enforced expression of GFP alone did not effect the morphology of the cells, and the GFP was diffusely localized throughout the cytoplasm and nucleus of the cell (Fig. 4A). Expression of GFP-mPIP5K-Iβ in 293T cells produced a large vesicle phenotype identical to that previously observed for the untagged protein (Fig. 4B left panel). Fluorescent microscopy revealed that the GFP-mPIP5K-Iβ chimera was localized to the inner

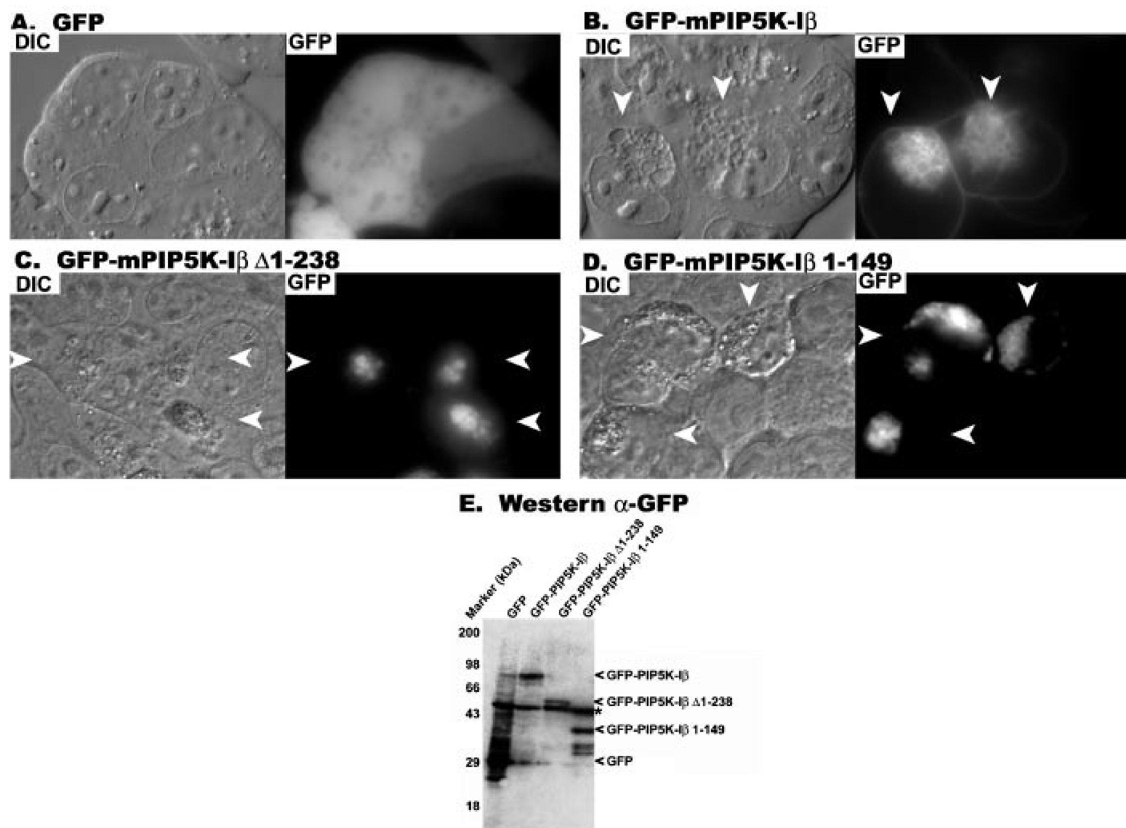

Fig. 4. Expression of GFP-mPIP5K-Iβ, GFP-mPIP5K-Iβ △1-238 GFP-and mPIP5K-Iβ 1-149 in 293T cells. **Panel A**: Photomicrographs obtained of 293T cells expressing GFP using DIC and fluorescent microscopy (GFP). **Panel B**: Photomicrographs obtained of 293T cells expressing GFP-mPIP5K-Iβ using DIC and fluorescent microscopy (GFP). The arrows indicate the transfected cells displaying the large vesicle phenotype. **Panel C**: Photomicrographs obtained of 293T cells expressing GFP-mPIP5K-Iβ △1-238 using DIC and fluorescent microscopy (GFP). The arrows indicate the transfected cells. **Panel D**: Photomicrographs obtained of 293T cells expressing GFP-mPIP5K-Iβ 1-149 using DIC and fluorescent microscopy (GFP). The arrows indicate the transfected cells. **Panel E**: Western analysis of extracts prepared from the cells expressing the tagged proteins (as indicated above the individual lanes). The arrows indicate the migration positions of the fusion proteins identified with antiserum to GFP. The asterisk indicates a non-specific band that reacts with this serum. The molecular mass markers are shown to the left.

surface of the plasma membrane and was associated with the surface of many of the large vesicles (Fig. 4B right panel). Thus, the GFP-chimera displayed the same localization as that observed for the untagged protein. Additionally, the kinase activity of GFP-mPIP5K-Iβ was tested in immune complex kinase assays and was equivalent to the untagged protein (data not shown). The non-transfected cells in the same field did not display the large vesicle phenotype or GFP fluorescence.

Our previous studies identified an N-terminal truncation of mPIP5K-Iβ (mPIP5K-Iβ △1-238) that was able to inhibit the downregulation of a ligand activated CSF-1R [Davis et al., 1997]. mPIP5K-Iβ △1-238 was subsequently shown to increase the nucleotide sensitivity of ATP-sensitive potassium channels [Shyng et al., 2000]. A GFP-fusion protein corresponding to mPIP5K-Iβ △1-238 was constructed and characterized in 293T cells. Additionally, a GFP-fusion protein containing the first 238 amino acids of mPIP5K-Iβ (GFP-mPIP5K-Iβ 1-238) was prepared and examined. Expression of GFP-mPIP5K-Iβ △1-238 in the 293T cells failed to induce the formation of the large vesicles (Fig. 4C). GFP-mPIP5K-Iβ △1-238 was not associated with plasma membrane but rather was distributed in the cytoplasm with a distinct granular pattern. GFP-mPIP5K-Iβ 1-238 also failed to induce the large vesicle phenotype, and the protein was distributed in the same cytoplasmic granular pattern that was observed for GFP-mPIP5K-Iβ △1-238 (data not shown). Since the crystal structure of the related PI5P4K-IIβ enzyme indicated that

the N-terminal region of the kinase contained a homodimerization domain, we hypothesized that dimerization and aggregation of the protein may be related to the granulated distribution of the protein. To begin to test this hypothesis, a smaller amino terminal fragment containing the putative dimerization domain of mPIP5K-Iβ was fused to GFP to create mPIP5K-Iβ 1-149 [Rao et al., 1998]. Expression of mPIP5K-Iβ 1-149 in 293T cells resulted in a similar localization pattern for that observed with GFP-1-238 and GFP-mPIP5K-Iβ △1-238 (Fig. 4D). These results are consisent with the hypothesis that the granulated localization of the proteins may be due in part to aggregation arising from the presence of dimerization domains.

Additional N- or C-terminal truncations were constructed and tested for the ability to induce the large vesicle phenotype in 293T cells, and the results are summarized in schematic form (Fig. 5). Deletion of the non-conserved N-terminal and C-terminal regions had no effect on kinase activity (GFP-59-439 “Core”), subcellular distribution or induction of the large vesicle phenotype. However, deletion into the conserved kinase core (GFP-△1-153 or GFP-1-368) resulted in the loss of the large vesicle phenotype and the proteins localized in a similar manner to GFP-mPIP5K-Iβ 1-149 and mPIP5K-Iβ△1-238. Co-expression of overlapping N- and C-terminal deletions in the 293T cells failed to induce the accumulation of the large vesicles, suggesting that the phenotype did not result from the expression of two separable domains within the protein. Thus, induction of the large vesicle phenotype required an intact kinase core domain that is highly conserved between the different type I isoforms, although kinase activity was not required.

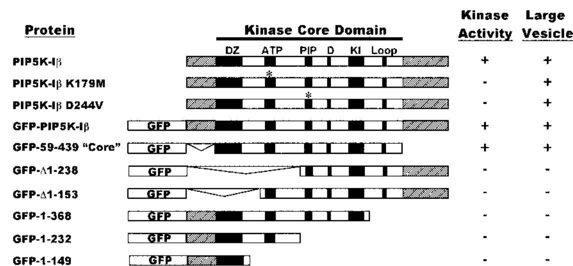

Fig. 5. Schematic representation of the phenotypes that resulted from the expression of various mPIP5K-Iβ derived proteins in 293T cells. Representations of the various proteins are presented as rectangles that were drawn to scale. The hatched areas at the ends represent the N- and C-terminal regions that are not conserved between the type I family of kinases. Important structural motifs were identified in the related PIP4K-IIβ structure and the corresponding regions of mPIP5K-Iβ are represented by the black rectangles. The abbreviations for these motifs are the following: DZ is the putative dimerization domain, ATP refers to the ATP-binding pocket, PIP was proposed to be a site of phosphatidylinositol binding, D refers to an aspartic acid residue that was proposed to serve as weak base in the catalysis, KI represents a kinase insert domain, and Loop refers to the activation loop of the kinase. The asterisks denote the location of the point mutations in the kinase inactive isoforms. The kinase activity and the ability of the proteins to induce the accumulation of large vesicles was determined after expression in 293T and is indicated to the right of the illustration using the plus or minus symbols.

In order to determine if mPIP5K-Iβ 1-149 and mPIP5K-Iβ △1-238 dimerize with mPIP5K-Iβ in vivo, chimeric proteins that contained the cyan fluorescent protein (CFP) fused to the N-terminus of mPIP5K-Iβ 1-149 and mPIP5K-Iβ △1-238 were expressed. Yellow fluorescent protein (YFP) was fused to the amino terminus of mPIP5K-Iβ in a similar fashion. CFP and YFP are isoforms of the GFP which display distinct absorption and emission spectra. Therefore, the fluorescence from the CFP and YFP can be distinguished by using appropriate excitation and emission filters following their co-expression in living cells. Similar analysis has been performed with interacting proteins by using proteins tagged with the blue fluorescent protein (BFP) and GFP [Day, 1998; Stauber et al., 1998; Yang et al., 1998] and using CFP and YFP with this particular microscope [Odaka et al., 2000].

Co-expression of YFP-mPIP5K-Iβ with CFP produced the large vesicle phenotype, and YFP-mPIP5K-Iβ properly localized to the plasma membrane and to the surface of the large vesicles (Fig. 6A). Under these conditions, the diffuse nuclear and cytoplasmic localization of CFP was observed only when using the CFP specific filters (Fig. 6A). Co-expression of YFP-mPIP5K-Iβ with either CFP-mPIP5K-Iβ △1-238 or CFP-mPIP5K-Iβ 1-149 altered the subcellular localization of the YFP-mPIP5K-Iβ (Fig. 6B,C). While some of the YFP-mPIP5K-Iβ localized to the plasma membrane, the majority of YFP-mPIP5K-Iβ co-localized with the CFP-mPIP5K-Iβ △1-238 (Fig. 6B) or CFP-mPIP5K-Iβ 1-149 (Fig. 6C). Thus, mPIP5K-Iβ 1-149 and mPIP5K-Iβ △1-238 expression altered the subcellular distribution of YFP-mPIP5K-Iβ and interfered with the accumulation of the large vesicles induced by the full-length protein.

To eliminate the possibility that the co-localization observed in vivo was due to non-specific aggregation of the proteins, direct interaction of soluble proteins was tested. Glutathione-S-transferase (GST)-fusion proteins of mPIP5K-Iβ, mPIP5K-IβI-149, and mPIP5K-Iβ △1-238 were produced in bacteria and purified by affinity chromatography using glutathione-Sepharose (Fig. 6D). These proteins were tested for their ability to associate with [^{35}S]-methionine-labeled mPIP5K-Iβ prepared by in vitro transcription and translation in GST-capture assay. [^{35}S]-methionine-labeled mPIP5K was incubated with the bacterially expressed proteins on glutathione-Sepharose beads and, after washing, the proteins were eluted from the beads, and subjected to SDS–PAGE and autoradiography (Fig. 6D). mPIP5K-Iβ formed stable complexes with both the products as well as the full-length protein. No binding to the GST control was observed. Thus, both the C-terminal and N-terminal globular domains of mPIP5K-Iβ displayed the ability to dimerize with the full-length enzyme in vitro.

mPIP5K-Iβ 1-149 and mPIP5K-Iβ △1-238 Alter PLC-δ-PH Localization

Since expression of mPIP5K-Iβ 1-149 or mPIP5K-Iβ △1-238 altered the subcellular distribution of mPIP5K-Iβ, we examined the affect that co-expression of these proteins had on the localization of the PLC-δ- and Btk-PH domains. Cells co-expressing high levels of PLC-δ-PH and mPIP5K-Iβ could not be obtained. Thus, the amount of YFP-PLC-δ-PH expression plasmid was reduced to limit PLC-δ-PH expression to levels that did not induce aberrant vesicle formation (Fig. 7A). Under these conditions, YFP-PLC-δ-PH displayed a plasma membrane staining pattern consistent with previous reports. Identical results were observed for CFP-PLC-δ-PH (data not shown). Co-expression of CFP-PLC-δ-PH with YFP-mPIP5K-Iβ shows that both proteins localized to the plasma membrane and to the surface of the large vesicles (Fig. 7B). This result was expected since expression of either protein individually displayed this subcellular localization. Co-expression of YFP-PLC-δ-PH with CFP-mPIP5K-Iβ 1-149 or CFP-mPIP5K-Iβ △1-238 resulted in co-localization of the PH domain with the truncated proteins (Fig. 7C,D). This result is consistent with the ability of the mPIP5K-Iβ 1-149 and mPIP5K-Iβ △1-238 to bind and alter the localization of the endogenous PI4P5K-Iβ enzyme. Thus, the subcellular distribution of PI (4,5) P_2 may be determined in part by the location of the PI4P5K enzyme.

The ability of mPIP5K-Iβ 1-149 and mPIP5K-Iβ △1-238 to alter the localization of the PH domain required PI (4,5) P_2-binding, since a different pattern of expression was observed following expression of the PtdIns(3,4,5)P_3-binding PH domain of Btk. Co-expression of YFP-BTK-PH with CFP demonstrated that the Btk-PH domain primarily localized to the plasma membrane but was also associated with an occasional small vesicle (Fig. 7E). In contrast to the PLC-PH domain, the Btk-PH domain did not co-localize with mPIP5K-Iβ (Fig. 7F). However, some of CFP-Btk-PH localized in a punctate pattern in the area of vesicle accumulation induced by YFP-mPIP5K-Iβ (Fig. 7F-CFP) and the membrane localization appeared to be decreased. This altered localization could reflect disruption of PI(3,4,5)P_3 regulated endocytic pathways or disruption of other PI (4,5) P_2 regulated pathways. Co-expression of YFP-BTK-PH with CFP-mPIP5K-Iβ 1-149 or CFP-mPIP5K-Iβ △1-238 had a much less dramatic effect on the localization of the Btk-PH domain (Fig. 5G,H). While some of the YFP-BTK-PH protein localized to the general area of the truncated mPIP5K-Iβ proteins, the majority of the YFP-BTK-PH was associated with the plasma membrane. We conclude that the PI(4,5) P_2-binding PH domain of PLC-δ co-localized with the mPIP5K-Iβ enzyme, whereas, the localization of the PI (3,4,5) P_3 binding Btk-Ph domain was independent of mPIP5K-Iβ.

DISCUSSION

This study demonstrates that enforced expression of high levels of mPIP5K-Iβ in 293T cells induced the accumulation of large vesicles associated with an endocytic pathway. mPIP5K-Iβ was localized to the surface of these vesicles that were found to contain markers of fluid phase pinocytosis and receptor mediated endocytosis. The induction of the large vesicles was independent of lipid kinase activity but required the entire kinase core domain. Interestingly, studies performed in COS cells have shown induction of aberrant actin polymerization by the type I mPIP5K isoforms [Shibasaki et al., 1997]. The induction of actin polymerization was also independent of kinase activity

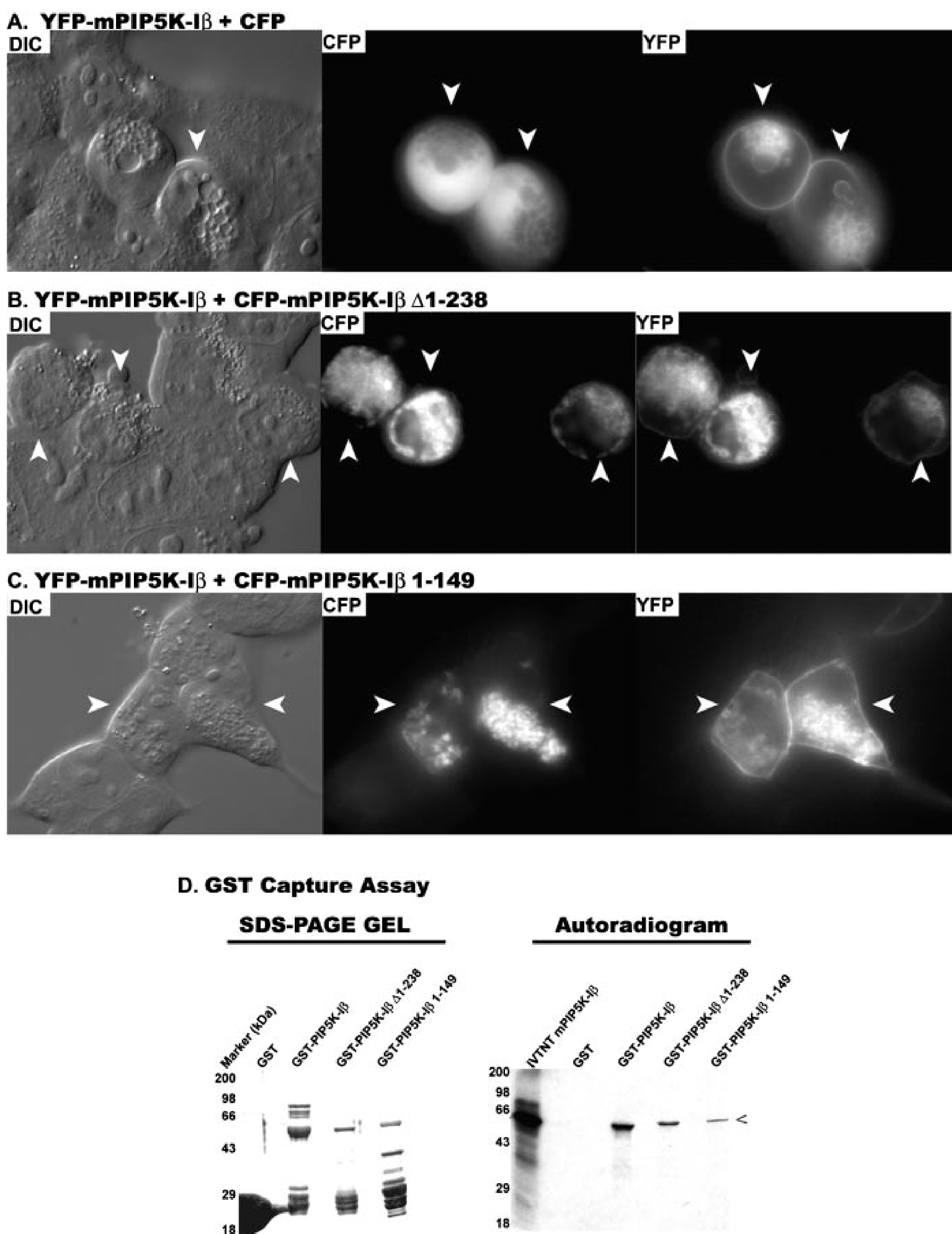

Fig. 6. YFP-mPIP5K-Iβ co-localizes with CFP-mPIP5K-Iβ △1-238 or CFP-mPIP5K-Iβ 1-149. 293T cells were co-transfected with vectors directing the synthesis of the proteins indicated above each panel, and the cells were photographed by using either DIC microscopy (DIC) or fluorescent microscopy with filters specific for YFP or CFP fluorescence as indicated. **Panel A**: Cells expressed YFP-mPIP5K-Iβ and CFP. **Panel B**: Cells expressed YFP-mPIP5K-Iβ and CFP-mPIP5K-Iβ △1-238. **Panel C**: Cells expressed YFP-mPIP5K-Iβ and CFP-mPIP5K-Iβ 1-149. The arrowheads in each panel designate cells that co-express the indicated proteins. **Panel D**: The GST fusion proteins were purified from bacteria by glutathionine–Sepharose and analyzed by SDS–PAGE and stained with Coomassie brilliant blue (SDS–PAGE Gel). The proteins are denoted above each lane. ^{35}S-methionine labeled mPIP5K-Iβ was incubated with the beads containing the GST products indicated, washed, and analyzed by SDS–PAGE and autoradiography (Autoradiogram). The migration position of mPIP5K-Iβ is indicted by the arrowhead at the right of the autoradiogram. The in vitro translated probe (IVTNT) is shown in the first lane.

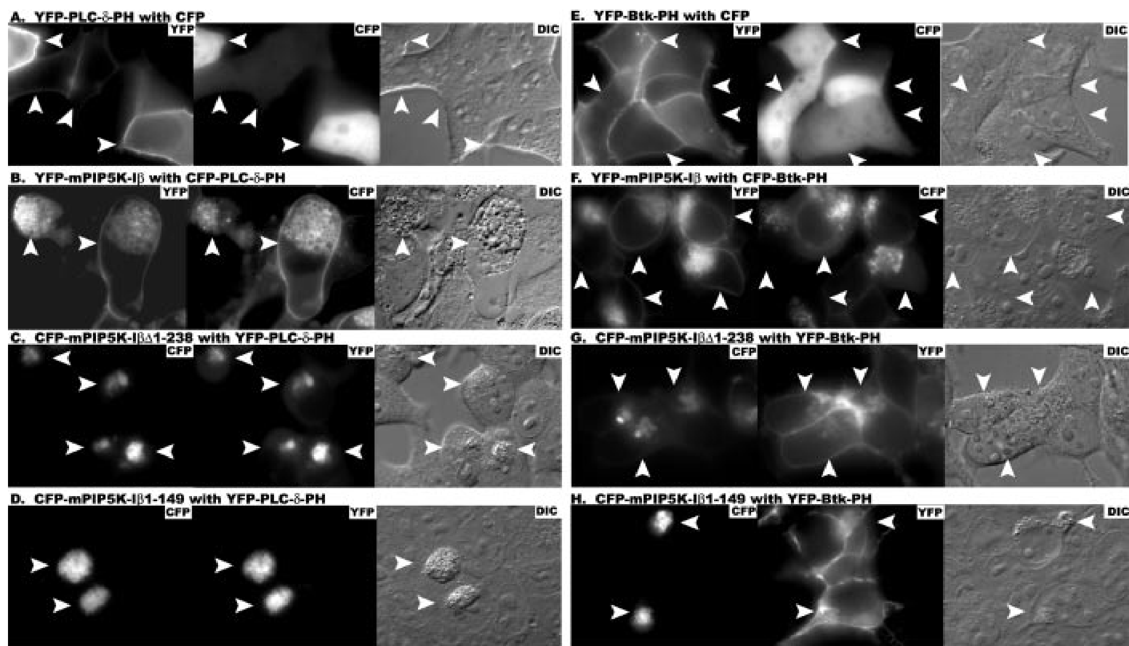

Fig. 7. mPIP5K-Iβ, PIP5K-Iβ △1-238, and PIP5K-Iβ 1-149 co-localize with the PI (4,5) P_2-binding PH-domain of PLC-δ but not the PI (3,4,5) P_3-binding PH-domain of Btk. 293T cells were transfected with vectors that direct the synthesis of the proteins indicated above each panel and DIC or fluorescent microscopy employing filters specific for YFP or CFP fluorescence was performed. **Panel A**: 293T cells were co-transfected with expression vectors encoding YFP-PLC-δ-PH and CFP were analyzed. **Panel B**: 293T cells co-expressing YFP-mPIP5K-Iβ and CFP-PLC-δ-PH were analyzed. **Panel C**: 293T cells co-expressing CFP-mPIP5K-Iβ △1-238 and YFP- PLC-δ-PH were analyzed. **Panel D**: 293T cells co-expressing CFP-mPIP5K-Iβ △1-149 and YFP-PLC-δ-PH were analyzed. **Panel E**: 293T cells co-transfected with expression vectors encoding YFP-BTK-PH and CFP were analyzed. **Panel F**: 293T cells co-expressing YFP-mPIP5K-Iβ and CFP-BTK-PH were analyzed. **Panel G**: 293T cells co-expressing CFP-mPIP5K-Iβ △1-238 and YFP-BTK-PH were analyzed. **Panel H**: 293T cells co-expressing CFP-mPIP5K-Iβ △1-149 and YFP-BTK-PH were analyzed.

and required the complete kinase core. Why overexpression of mPIP5K-Iβ induces aberrant vesicle accumulation in one system and predominantly effects the actin cytoskeleton in another is not clear. However, results similar to those described in this report provide evidence that activated ARF6 (a small G-protein tied to receptor mediated endocytosis, vesicle trafficking, and membrane ruffling) and human PIP5K-Iα induced the accumulation of vacuoles derived from an endosomal compartment responsible for membrane recycling [Brown et al., 2001]. The mechanism by which overexpression of the type I PIP5Ks disrupts the endosomal trafficking is yet to be fully elucidated and may involve the titration of cellular factors or the dysregulation of PI (4,5) P_2 synthesis or localization.

Deletions into the conserved kinase core of mPIP5K-Iβ disrupted the ability of the protein to induce the acculumation of the large vesicles and the truncated proteins displayed a propensity for aggregation upon enforced expression in the 293T cells. While the aggregation could result from mis-folding, the ability of the proteins to dimerize may also be a contributing factor. Moreover, co-expression mPIP5K-β △1-238 and mPIP5K-β 1-238 blocked the ability of mPIP5K-Iβ to induce the large vesicles and altered the subcellular distribution of the wild-type protein. mPIP5K-Iβ △1-238 was isolated through its ability to restore the mitogenic capacity to a compromised CSF-1R [Davis et al., 1997], suggesting that the truncation generated a protein with a dominant-negative function toward mPIP5K-Iβ regulated pathways. It was proposed that mPIP5K-Iβ △1-238 blocked the ligand-dependent internalization of the receptor allowing sufficient time for the crippled receptor to activate proliferative pathways. This report provides evidence that the proposed dominant-negative activity of mPIP5K-Iβ △1-238 may be mediated through direct binding to mPIP5K-Iβ. mPIP5K-Iβ also formed stable complexes with the fusion proteins containing the N-terminus (mPIP5K-Iβ

1-149), indicating that at least two separate regions in mPIP5K-Iβ mediate self-association. The presence of two independent dimerization domains within mPIP5K-Iβ provides the potential for the formation of oligomeric protein complexes. Gel filtration analysis revealed that mPIP5K-Iβ is present in high molecular weight protein complex(es) (data not shown). Release of the active enzyme from such oligomeric complexes could provide a physiological mechanism to regulate mPIP5K-Iβ activity. It remains to be determined how the isolated dimerization domains alter the distribution of mPIP5K-Iβ. It has been suggested that dimerization of PI5P4K-IIβ is required to form a positively charged surface that could interact with the negatively charged membrane [Rao et al., 1998]. If a similar mechanism was invoked for the type I enzymes, the overexpression of the isolated dimerization domains would be expected to disrupt membrane association. A previous study suggested that the putative activation loop of the type I and II kinases was also involved in determining the subcellular distribution the individual kinases [Kunz et al., 2000]. Thus, the proper localization of the type I PIP5Ks may be complex, requiring dimerization and other lipid binding domains.

Studies presented here indicate that the induction of the large vesicle phenotype by mPIP5K-Iβ could be blocked by co-expression of the fusion proteins containing either the N-or C-terminal regions of the protein. A similar response was observed following co-expression of the truncated proteins with the PH domain of PLC-δ (a domain that specifically binds PI $(4,5)P_2$). Though not shown directly, it is likely that PLC-PH binds PI $(4,5)P_2$ in intact cells and that the truncated proteins not only block mPIP5K-Iβ association with the plasma membrane but also alter the subcellular distribution of $PI(4,5)P_2$. These proteins may, therefore, provide important tools to dissect plasma membrane activities that are dependent upon localized PI $(4,5)P_2$.

ACKNOWLEDGMENTS

The authors thank Shari Meyers and Jim Cardelli for helpful discussions, Kelly Tatchell for permitting the extensive use of the microscope, Tamas Balla for the generous gift of the PLC-δ and Btk PH-domains, and Nam-Hai Chua for the PLC-δ Ph domain mutant.

REFERENCES

Brown FD, Rozelle AL, Yin HL, Balla T, Donaldson JG. 2001. Phosphatidylinositol 4,5-bisphosphate and Arf6-regulated membrane traffic. J Cell Biol 154:1007–1017.

Burnette WN. 1981. Western blotting: electrophoretic transfer of proteins from sodium dodecyl sulfate–polyacrylamide gels to unmodified nitrocellulose and radiographic detection with antibody and radioiodinated protein A. Anal Biochem 112:195–203.

Chen C, Okayama H. 1987. High-efficiency transformation of mammalian cells by plasmid DNA. Mol Cell Biol 7: 2745–2452.

Davis JN, Rock CO, Cheng M, Watson JB, Ashmun RA, Kirk H, Kay RJ, Roussel MF. 1997. Complementation of growth factor receptor-dependent mitogenic signaling by a truncated type I phosphatidylinositol 4-phosphate 5-kinase. Mol Cell Biol 17:7398–7406.

Day RN. 1998. Visualization of Pit-1 transcription factor interactions in the living cell nucleus by fluorescence resonance energy transfer microscopy. Mol Endocrinol 12: 1410–1419.

Ford MG, Pearse BM, Higgins MK, Vallis Y, Owen DJ, Gibson A, Hopkins CR, Evans PR, McMahon HT. 2001. Simultaneous binding of PtdIns(4,5)P2 and clathrin by AP180 in the nucleation of clathrin lattices on membranes. Science 291:1051–1055.

Gillooly DJ, Stenmark H. 2001. Cell biology. A lipid oils the endocytosis machine. Science 291:993–994.

Hinchliffe KA, Ciruela A, Irvine RF. 1998. PIPkins1, their substrates and their products: new functions for old enzymes. Biochim Biophys Acta 1436:87–104.

Ishihara H, Shibasaki Y, Kizuki N, Katagiri H, Yazaki Y, Asano T, Oka Y. 1996. Cloning of cDNAs encoding two isoforms of 68-kDa type I phosphatidylinositol-4-phosphate 5-kinase. J Biol Chem 271:23611–23614.

Ishihara H, Shibasaki Y, Kizuki N, Wada T, Yazaki Y, Asano T, Oka Y. 1998. Type I phosphatidylinositol-4-phosphate 5-kinases. Cloning of the third isoform and deletion/substitution analysis of members of this novel lipid kinase family. J Biol Chem 273:8741–8748.

Itoh T, Koshiba S, Kigawa T, Kikuchi A, Yokoyama S, Takenawa T. 2001. Role of the ENTH domain in phosphatidylinositol-4,5-bisphosphate binding and endocytosis. Science 291:104–751.

Kost B, Lemichez E, Spielhofer P, Hong Y, Tolias K, Carpenter C, Chua NH. 1999. Rac homologues and compartmentalized phosphatidylinositol 4, 5 bisphosphate act in a common pathway to regulate polar pollen tube growth. J Cell Biol 145:317–330.

Kunz J, Wilson MP, Kisseleva M, Hurley JH, Majerus PW, Anderson RA. 2000. The activation loop of phosphatidylinositol phosphate kinases determines signaling specificity. Mol Cell 5:1–11.

Laemmli UK. 1970. Cleavage of structural proteins during the assembly of the head of bacteriophage T4. Nature 227:680–685.

Loijens JC, Boronenkov IV, Parker GJ, Anderson RA. 1996. The phosphatidylinositol 4-phosphate 5-kinase family. Adv Enzyme Regul 36:115–140.

Odaka Y, Mally A, Elliott LT, Meyers S. 2000. Nuclear import and subnuclear localization of the proto-oncoprotein ETO (MTG8). Oncogene 19:3584–3597.

Rameh LE, Tolias KF, Duckworth BC, Cantley LC. 1997. A new pathway for synthesis of phosphatidylinositol-4,5-bisphosphate. Nature 390:192–196.
Rao VD, Misra S, Boronenkov IV, Anderson RA, Hurley JH. 1998. Structure of type IIbeta phosphatidylinositol phosphate kinase: a protein kinase fold flattened for interfacial phosphorylation. Cell 94:829–839.
Shibasaki Y, Ishihara H, Kizuki N, Asano T, Oka Y, Yazaki Y. 1997. Massive actin polymerization induced by phosphatidylinositol-4-phosphate 5-kinase in vivo. J Biol Chem 272:7578–7581.
Shyng SL, Barbieri A, Gumusboga A, Cukras C, Pike L, Davis JN, Stahl PD, Nichols CG. 2000. Modulation of nucleotide sensitivity of ATP-sensitive potassium channels by phosphatidylinositol-4-phosphate 5-kinase. Proc Natl Acad Sci 97:937–941.
Stauber RH, Horie K, Carney P, Hudson EA, Tarasova NI, Gaitanaris GA, Pavlakis GN. 1998. Development and applications of enhanced green fluorescent protein mutants. Biotechniques 24:462–466.
Stauffer TP, Ahn S, Meyer T. 1998. Receptor-induced transient reduction in plasma membrane PtdIns(4,5)P2 concentration monitored in living cells. Curr Biol 8:343–346.
Stephens LR, Hughes KT, Irvine RF. 1991. Pathway of phosphatidylinositol(3,4,5)-trisphosphate synthesis in activated neutrophils. Nature 351:33–39.
Tuma PL, Stachniak MC, Collins CA. 1993. Activation of dynamin GTPase by acidic phospholipids and endogenous rat brain vesicles. J Biol Chem 268:17240–17246.
Ulug ET, Hawkins PT, Hanley MR, Courtneidge SA. 1990. Phosphatidylinositol metabolism in cells transformed by polyomavirus middle T antigen. J Virol 64:3895–3904.
Varnai P, Balla T. 1998. Visualization of phosphoinositides that bind pleckstrin homology domains: calcium- and agonist-induced dynamic changes and relationship to myo-[3H]inositol-labeled phosphoinositide pools. J Cell Biol 143:501–510.
Varnai P, Rother KI, Balla T. 1999. Phosphatidylinositol 3-kinase-dependent membrane association of the Bruton's tyrosine kinase pleckstrin homology domain visualized in single living cells. J Biol Chem 274:10983–10989.
Yang TT, Sinai P, Green G, Kitts PA, Chen YT, Lybarger L, Chervenak R, Patterson GH, Piston DW, Kain SR. 1998. Improved fluorescence and dual color detection with enhanced blue and green variants of the green fluorescent protein. J Biol Chem 273:8212–8216.